Journal of Power Sources 188 (2009) 205–212

Contents lists available at ScienceDirect

Journal of Power Sources

journal homepage: www.elsevier.com/locate/jpowsour

Operational condition analysis for vapor-fed direct methanol fuel cells

Ikwhang Chang[a,d], Seungbum Ha[b,d], Sunghan Kim[b], Sangkyun Kang[c], Jinho Kim[c], Kyounghwan Choi[c], Suk Won Cha[b,d,*]

[a] Interdisciplinary Program in Automotive Engineering, Seoul National University, San 56-1, Sillim9-dong, Kwanak-gu, Seoul 151-744, Republic of Korea
[b] Department of Mechanical and Aerospace Engineering, Seoul National University, San 56-1, Sillim9-dong, Kwanak-gu, Seoul 151-744, Republic of Korea
[c] Samsung Advanced Institute of Technology, San 14-1, Nongseo-Dong, Giheung-Gu, Yongin-Si, Gyeonggi-do 449-712, Republic of Korea
[d] Institute of Advanced Machinery and Design, Seoul National University, San 56-1, Sillim9-dong Kwanak-gu, Seoul 151-744, Republic of Korea

ARTICLE INFO

Article history:
Received 7 October 2008
Received in revised form
14 November 2008
Accepted 14 November 2008
Available online 24 November 2008

Keywords:
Direct methanol fuel cell
Reference electrode
Activation loss
Impedance
Air-breathing
Vapor-feeding

ABSTRACT

This paper investigates the analysis and design of optimal operational conditions for vapor-fed direct methanol fuel cells (DMFCs). Methanol vapor at a temperature of 35 °C is carried with nitrogen gas together with water vapor at 75 °C. In this experimental condition, stoichiometry of 10 is maintained for each fuel gas. The results show that the optimal operational concentration was 25–30 wt.% under methanol vapor feeding at the anode. The peak power was 14 mW cm^2 in polarization curves. To analyze major losses, the activation losses of the anode and cathode were measured by an in situ reference electrode and a working electrode. The activation loss of the anode is proportional to the water content and the high methanol concentration caused the activation loss of the cathode to increase due to methanol crossover. In the vapor-fed DMFC, the activation loss of the anode is higher than that of the cathode. Also, depending on the variation of the methanol concentration, the IR loss and Faradaic impedance is measured via impedance analysis. The methanol concentration significantly affects the IR loss and kinetics. Although the IR loss was more than the desired value at the optimal condition (25–30 wt.%), it did not significantly affect the cell's performance. The cell operated at room temperature and ambient pressure that is a typical operation environment of air-breathing fuel cells.

1. Introduction

Direct methanol fuel cells (DMFCs) are strong candidates for future portable power sources for cell phones, laptops, and MP3 players. DMFCs have many advantages as a portable power sources; low temperature operation, convenient storage of fuel, low emission pollutants, and high energy density (6100 kW kg^{-1}) [1–3]. The high energy density of methanol maximizes the operational life-time of the fuel cell from the limited volume of the fuel cartridge. Generally, liquid methanol is easy to store in the system, and DMFCs can operate at room temperature and ambient pressure, which is a significant advantage for portable applications [4–6]. In spite of these many advantages, DMFCs still have many difficult technological obstacles: high catalyst loading, the structure of electrode, CO poisoning of the triple phase boundary, slow electrochemical kinetics at the anode, methanol crossover through membrane and so on [7–9].

Eccarius et al. have supposed that methanol crossover relies strongly on temperature, membrane thickness, and methanol concentration. The analysis also revealed how these parameters influence the methanol crossover due to the effects on the methanol diffusion through the membrane, electro-osmotic drag, and the reaction rates of the methanol at the anode and cathode by several methods [7]. Reichman et al. investigated the novel PTFE-based proton conductive membrane. To reduce CO poisoning and crossover, they have developed and studied a solid polymer electrolyte operating above 130 °C and its membrane electrode assembly (MEA), with a 250 μm thick membrane, has been assembled demonstrate that 50 and 130 mW cm^2 could be produced at 80 and 130 °C, respectively [10].

In active fuel cells, the fuel is normally delivered by pump, or pressurized storage at the anode, and the air is usually supplied by blower at the cathode. Although active fuel cells have good performances, their parasite losses are inevitable due to the power consumption of pumps. In contrast to the active fuel cell, a passive fuel cell does not need any devices for delivering the fuel. Therefore, the volume of fuel delivery system can be reduced significantly. This gives a major advantage for portable applications using passive DMFCs. In passive fuel-feed DMFCs, the fuel can be fed in liquid or vapor form. Vapor-fed DMFCs can decrease methanol crossover compared with the liquid-fed ones [11,5].

* Corresponding author at: 301-1417, Seoul National University, Sillim9-dong, Kwanak-gu, Seoul 131-1744, Republic of Korea. Tel.: +82 2 8801700; fax: +82 2 8831513.
E-mail address: swcha@snu.ac.kr (S.W. Cha).

0378-7753/$ – see front matter.
doi:10.1016/j.jpowsour.2008.11.058

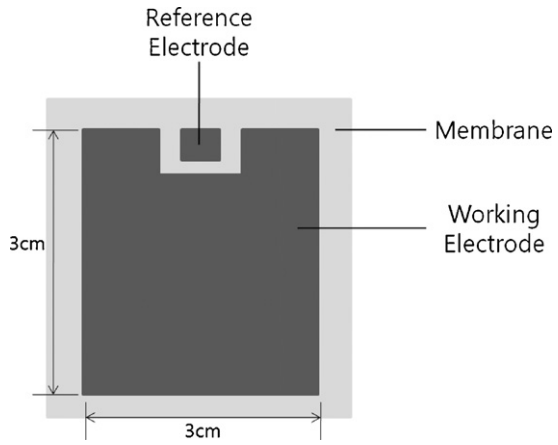

Fig. 1. Specification of reference electrode and working electrode.

Adler et al. revealed that the potential difference of the ionomer affects the accuracy between a working electrode and a reference electrode; the work shows that the geometries and locations of the reference electrode were critical issues [12]. The dynamic hydrogen electrode (DHE) is very useful as a reference electrode in PEM fuel cells [13,14].

In this paper, we investigate the optimal methanol concentration of a vapor-fed air breathing DMFC. To analyze major losses in fuel cells, we use an in situ reference electrode and impedance analysis. DMFC polarization curves were measured under various methanol concentrations from 15 to 40 wt.%. The relative activation losses were measured through a reference electrode. In the electrochemical impedance spectroscopy (EIS), we identified the IR loss, the Faradaic impedance and the mass transport effect.

2. Experimental

2.1. MEA preparation

The dimension of the MEA is 9 cm^2 (3 cm × 3 cm). The dimension of the reference electrode is 16 mm^2 (4 mm × 4 mm) and the layout is shown in Fig. 1. Both the anode and the cathode sides have the same reference electrode configuration. The electrolyte membrane was fabricated by a solution casting method having the thickness of 50 μm [15]. PtRu black and Pt black were used as the catalyst for the anode and the cathode, respectively. The catalyst loadings for the anode and cathode catalyst layers were 8 mg cm^{-2}.

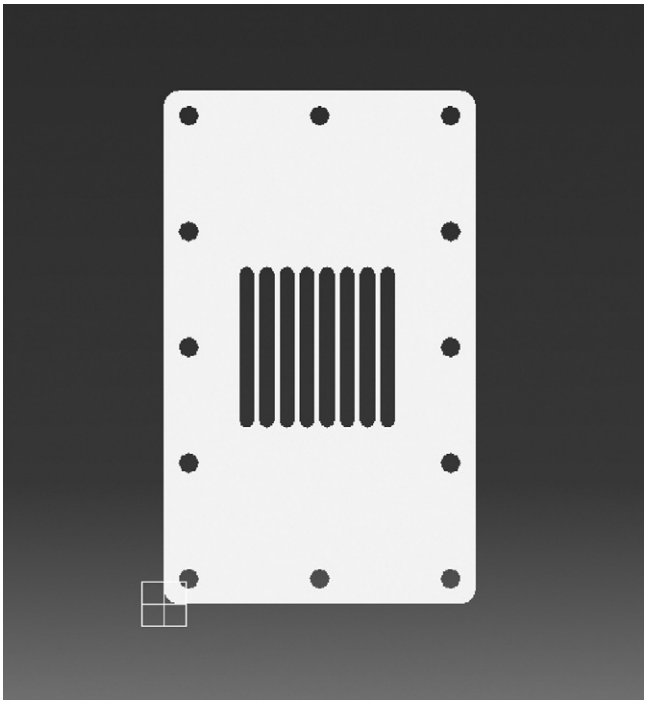

Fig. 2. Cathode plate design (Opening ratio 90%).

The anode diffusion layer was made of a carbon backing layer with silica particles of 4–5 nm and polyvinyldiene fluoride (PVDF). For the cathode diffusion layer, a mixture of carbon particles and polytetrafluoro ethylene (PTFE) was first sprayed onto the carbon backing layer with a loading of 2 mg cm^{-2}. SGL plain paper and Toray 090 carbon paper were used as the anode backing layers and for the cathode backing layer, respectively. Gold-coated nickel-mesh integrated with MEA was used as the current collector [15,16]. This current collector is embedded between the catalyst layer (CL) and the gas diffusion layer (GDL) to promote intimate contact and reduce ohmic resistance.

2.2. Cell assembly

The cell structure is made of polycarbonate. The dimension of the chamber used for mixing the fuel is 3 cm × 3 cm × 0.2 cm in the flow channel. The air is delivered by natural convection through the cathode holes of an opening ratio 90% (Fig. 2). The opening ratio of

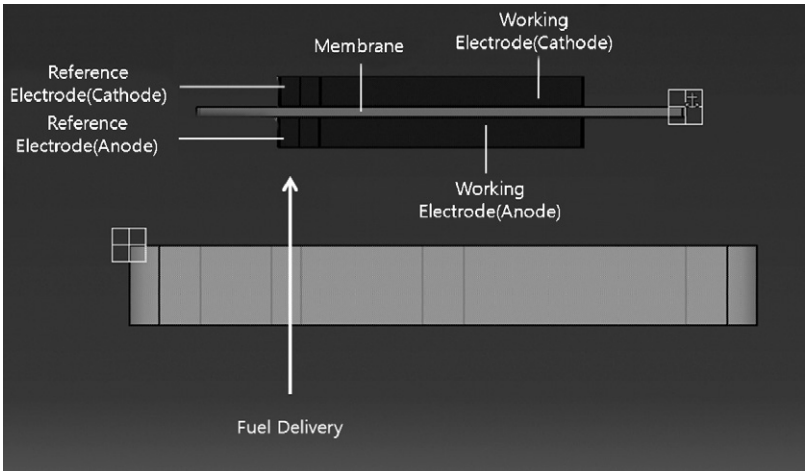

Fig. 3. The positions of fuel inlet and MEA (Side View).

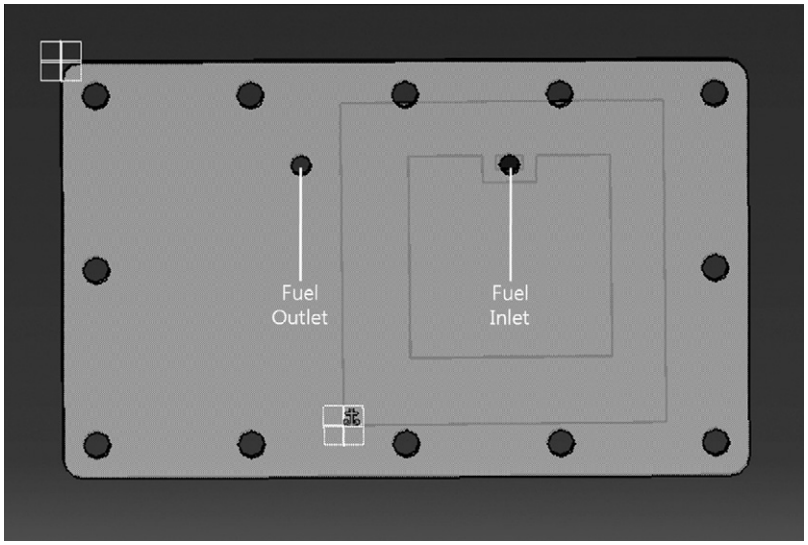

Fig. 4. The positions of fuel inlet and MEA (Top View).

the cathode is defined as follows:

$$\text{Opening ratio} = \frac{\text{Opened area}}{\text{Total area}} \quad (1)$$

The gasket thickness is 400 μm for both the cathode and the anode sides. The inlet position for the methanol supply is adjacent to the reference electrode as shown in Figs. 3 and 4.

2.3. Setup and measurement

Fig. 5 shows the methanol and water mixing mechanism to deliver nitrogen-carried vapor fuel to the fuel cell. The temperatures (wet bulb) of the water and methanol bath were maintained at 69 and 29 °C, respectively, on the hot plate. Before both the gases entered the cell, the final temperatures (dry bulb) of the water and methanol gases were fixed at 75 and 35 °C, respectively, using line heaters. The stoichiometry of both gases was 10. The mixed gases of methanol and water actively entered the membrane electrode assembly in the cell. Redundant gases drain via the outlet port. The oxygen is delivered to the gas diffusion layer of the cathode through natural convection. The experiment was carried out at room temperature and ambient pressure.

Polarization curve measurements were repeated several times to obtain steady-state performances. The polarization curves were obtained using a Solartron 1287 and a 1260 impedance/Gain-Phase Analyzer. Also, the AC impedance was measured using the same equipment. Impedance data were measured under DC load of 0.4 V, 0.3 V, and 0.2 V to investigate low, medium, and high current density response, respectively. The operational voltage of this fuel cell fluctuates widely due to unstable air and fuel supply in air-breathing and vapor-fed DMFCs. In particular, the voltage fluctuation is more prominent in a high current region. We could not measure any meaningful impedance spectra with typical signal amplitude (10–30 mV) because the noise (voltage fluctuation) is too high. In the experiment, a high amplitude value of 100 mV was employed to overcome this issue. The validity of such high amplitude value will be discussed later with the experimental result.

In the cell operating condition, the in situ reference electrode measured the relative activation loss between the working and the reference electrodes. The total polarization losses can be presented as follows [17]:

$$\eta_{\text{total}} = \eta_{\text{anode}} + \eta_{\text{ohmic}} + \eta_{\text{cathode}} = U_{\text{ref}} - U(I) \quad (2)$$

where η_{anode} is the anode activation loss, η_{cathode} is the cathode activation loss, and η_{ohmic} is the IR loss. U_{ref} is the open-circuit voltage (OCV) of the cell, and $U(I)$ is the actual voltage [18]. To find η_{anode}, a relative value of potential between the reference electrode of the anode and the working electrode of the anode was measured as shown in Fig. 6. In a similar method, we measured a relative value

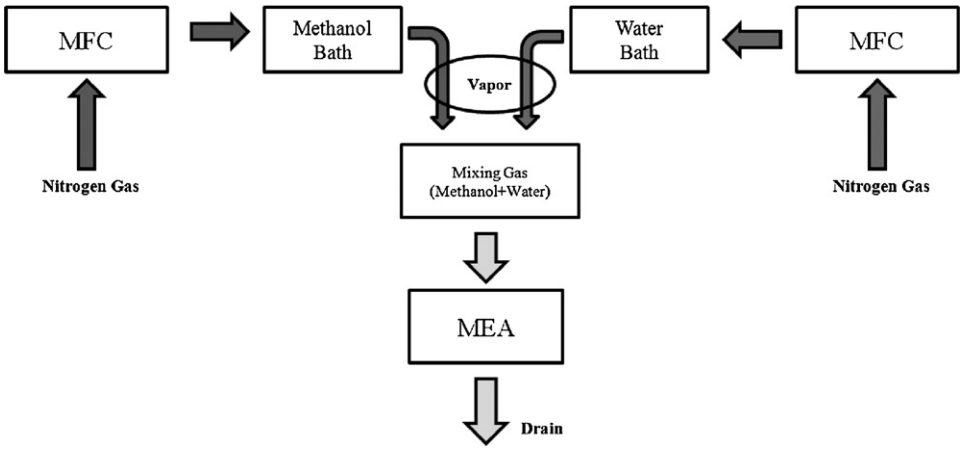

Fig. 5. Schematic of experimental setup.

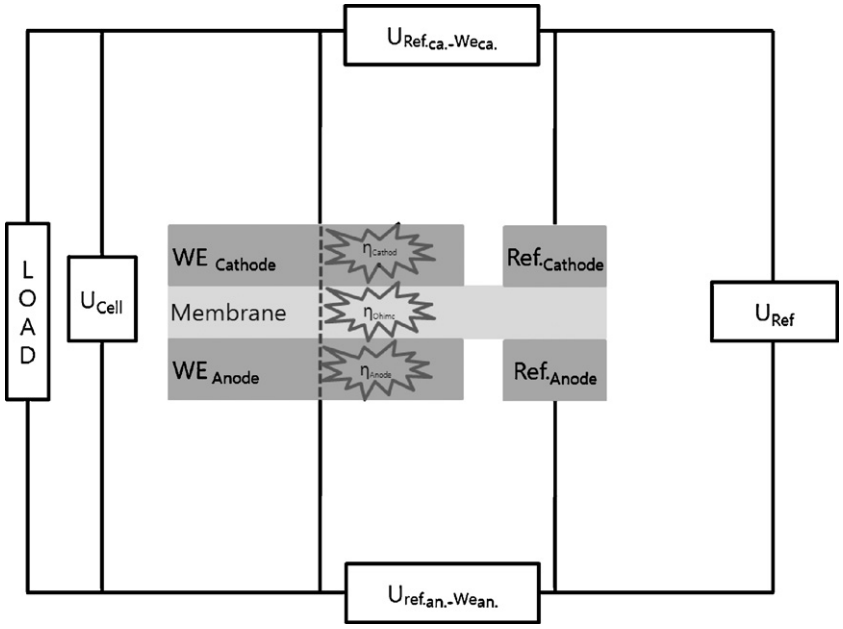

Fig. 6. Equivalent circuit of a fuel cell including a reference electrode: $\eta_{total} = \eta_{anode} + \eta_{ohmic} + \eta_{cathode} = U_{ref} - U(I)$.

of potential between the reference electrode of the cathode and the working electrode of the cathode. In contrast with the ex situ reference using dynamic hydrogen electrode (DHE), the boundary effects are negligible in the in situ reference electrode in order to minimize concentration losses. This indicates that finding the optimal geometric position is a complicated problem to maintain the same open-circuit voltage (OCV) between the working and the reference electrodes for in situ experiments [19].

3. Results and discussion

3.1. Effect of methanol concentration

Fig. 7 shows the open-circuit voltage (OCV) variation for 1300 s under various methanol concentrations. After 800 s, the OCV reaches a steady-state value. The OCV values of 30, 35, and 40 wt.% methanol concentration are similar, Therefore, we may conclude that the effect of methanol concentration on OCV is more dominant for dilute methanol (when the concentration is less than 30 wt.%). We obtained the best polarization curve when the methanol concentration is 25–30 wt.% that may be the optimal methanol concentration, as shown in Fig. 8. When the concentration is over 30 wt.%, due to high methanol crossover, the performance decreases gradually. In the optimal concentration, the peak power is 14 mW cm^2. The performances dependency on fuel concentration in vapor-fed DMFCs are similar to the methanol liquid feeding [20,21]. Interestingly, the optimal concentration of methanol in vapor-fed DMFCs was slightly higher than that of liquid-fed DMFCs. The optimal concentration difference may be attributed to two factors. The first is due to the low vapor pressure at the anode catalyst layer. Although the optimal methanol concentration is 25–30 wt.% (nominal concentration) in a reservoir, real concentration of the anode catalyst layer is much lower due to low vapor pressure at the experimental temperature. Thus, the solution concentration should be higher than the one of liquid fed DMFCs. Because the fuel in the vapor-fed DMFC has a low partial pressure, the fuel diffusion flux is also low from the flow channel to the catalyst layer. Therefore, in order to operate a fuel cell, a higher methanol concentration is needed to compensate the decreased methanol vapor pressure. The second factor is an increased methanol crossover in the cell due to the high temperature of the fuel gas [7]. In order to maintain enough partial pressure of fuel, the fuel temperature for vapor-fed should be higher than one for liquid-fed. Thus, increasing temperature of the MEA slightly increases the methanol crossover rate, thus further increasing the cell temperature, which reduces the potential difference at both the anode and the cathode [21–23]. However, the higher concentration than the optimal value causes the methanol crossover to deteriorate the cell performance by generating a mixed potential and poisoning the catalyst in the cathode. Therefore, over 6 mol methanol concentration would result in

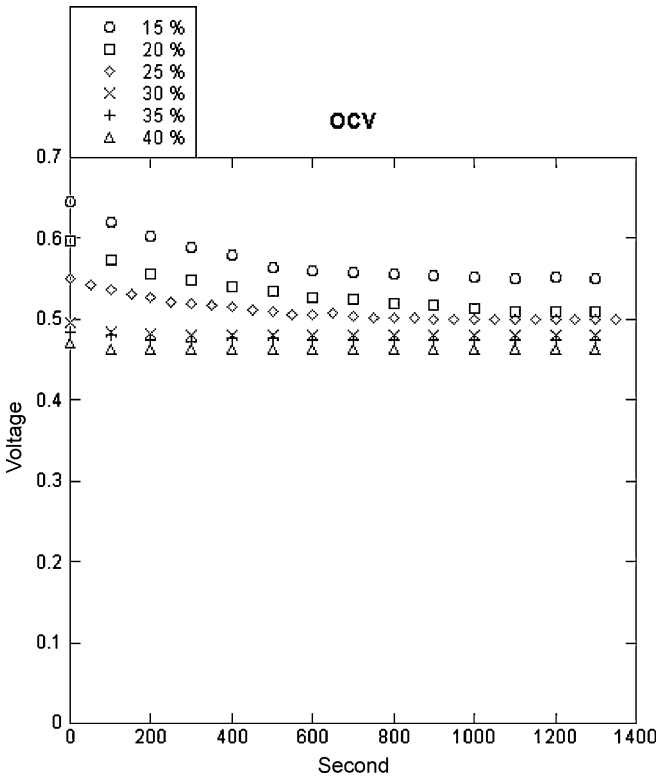

Fig. 7. OCV curves in different methanol concentrations.

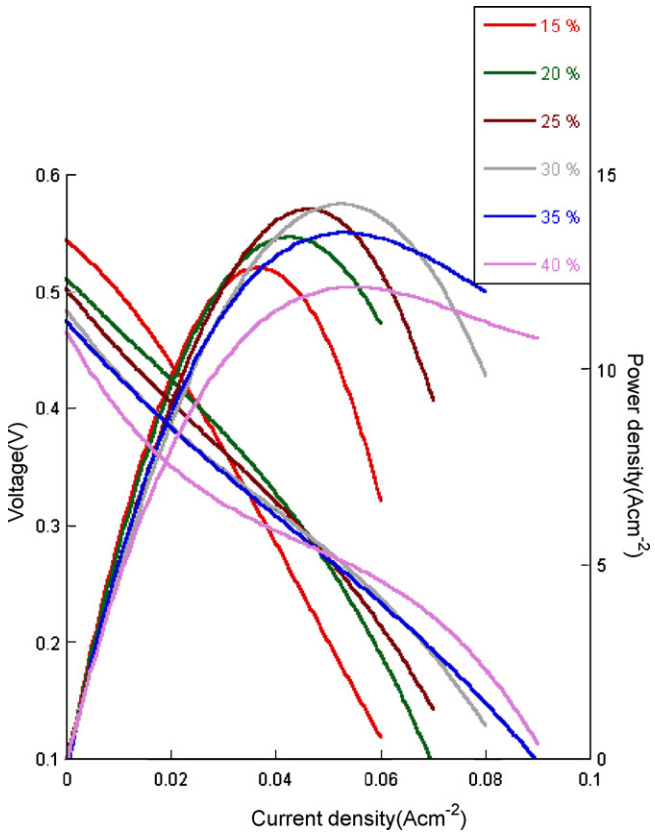

Fig. 8. Polarization curves in different methanol concentrations.

performance degradation due to the increased overpotential at the cathode [20].

3.2. Anode activation loss

Fig. 9 shows the relative potential difference between the reference electrode and the working electrode at the anode. High

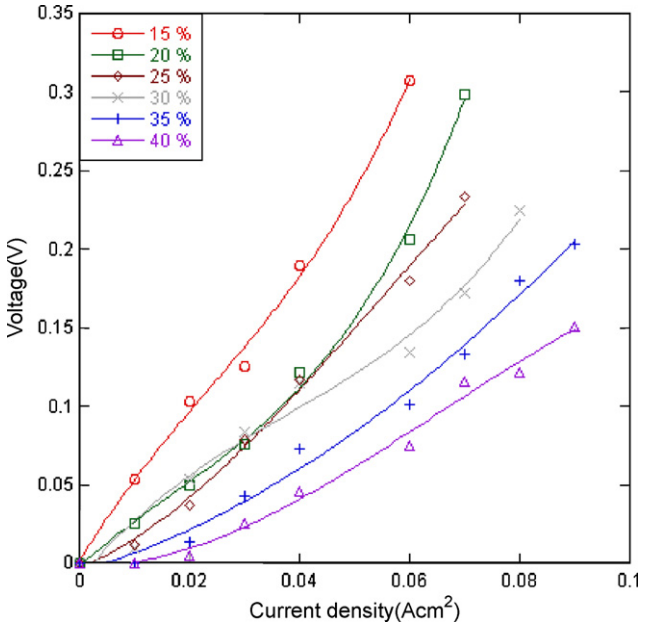

Fig. 9. Activation losses different methanol concentrations at the anode.

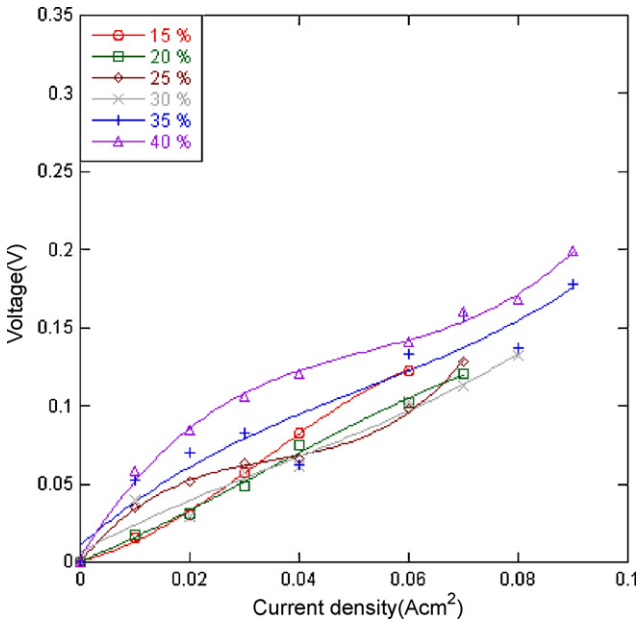

Fig. 10. Activation losses in different methanol concentrations at the cathode.

methanol concentration promotes the electrochemical kinetics at the anode. Especially, at the 0.04 A cm^2, the activation loss of the anode decreases as the following: 0.19 V (15%), 0.122 V (20%), 0.117 V (25%), 0.115 V (30%), 0.07 V (35%), and 0.05 V (40%). Accordingly, the activation losses of the anode are dominant for the low concentration levels. Conversely, the activation losses of the cathode are dominant for high concentration levels as shown in Fig. 10. Also, the activation losses of the anode increases when the current increases. The activation loss of the anode can be calculated as follows [24]:

$$\eta_{\text{anode}} = \frac{RT_{\text{acl}}}{6\alpha F} \ln \frac{J}{J_0} P^{\text{C}} X_{\text{MeOH}} \tag{3}$$

where η_{anode} is the anode activation loss, J_0 and P^{C} represent the reference exchange current density on the anode and the total pressure, X_{MeOH} is the methanol mole fraction in the anode catalyst layer, R is gas constant, T_{acl} is temperature of anode catalyst layer, α is transfer coefficient, and F is Faraday constant. In order to decrease the activation loss of the anode, the methanol concentration should sustain low methanol concentration loss between flow channel and anode catalyst layer. Thus, the high methanol concentration is more effective at the anode. The anode activation losses include IR losses such as membrane resistance and contact resistance. The IR losses should be deducted from anode activation losses. Reasonably, among activation losses, the anode activation loss can be calculated as this equation [18].

$$\eta_{\text{anode}} = U_{\text{ref-an}} - \frac{R^{\text{I}}_{\text{ohm}}}{2} \tag{4}$$

$U_{\text{ref-an}}$ stands for potential of the anode versus the OCV. Because of a homogeneous potential distribution within membrane, the deduction of half of the IR losses was reasonable [18]. Although the IR loss

Table 1
IR loss comparisons in different concentrations and applied voltages.

Concentration	0.2 V	0.3 V	0.4 V
15%	0.0616	0.0617	0.0620
20%	0.0616	0.0618	0.0621
25%	0.0640	0.0644	0.0645
30%	0.0642	0.0651	0.0643
35%	0.0678	0.0695	0.0680
40%	0.0720	0.0727	0.0719

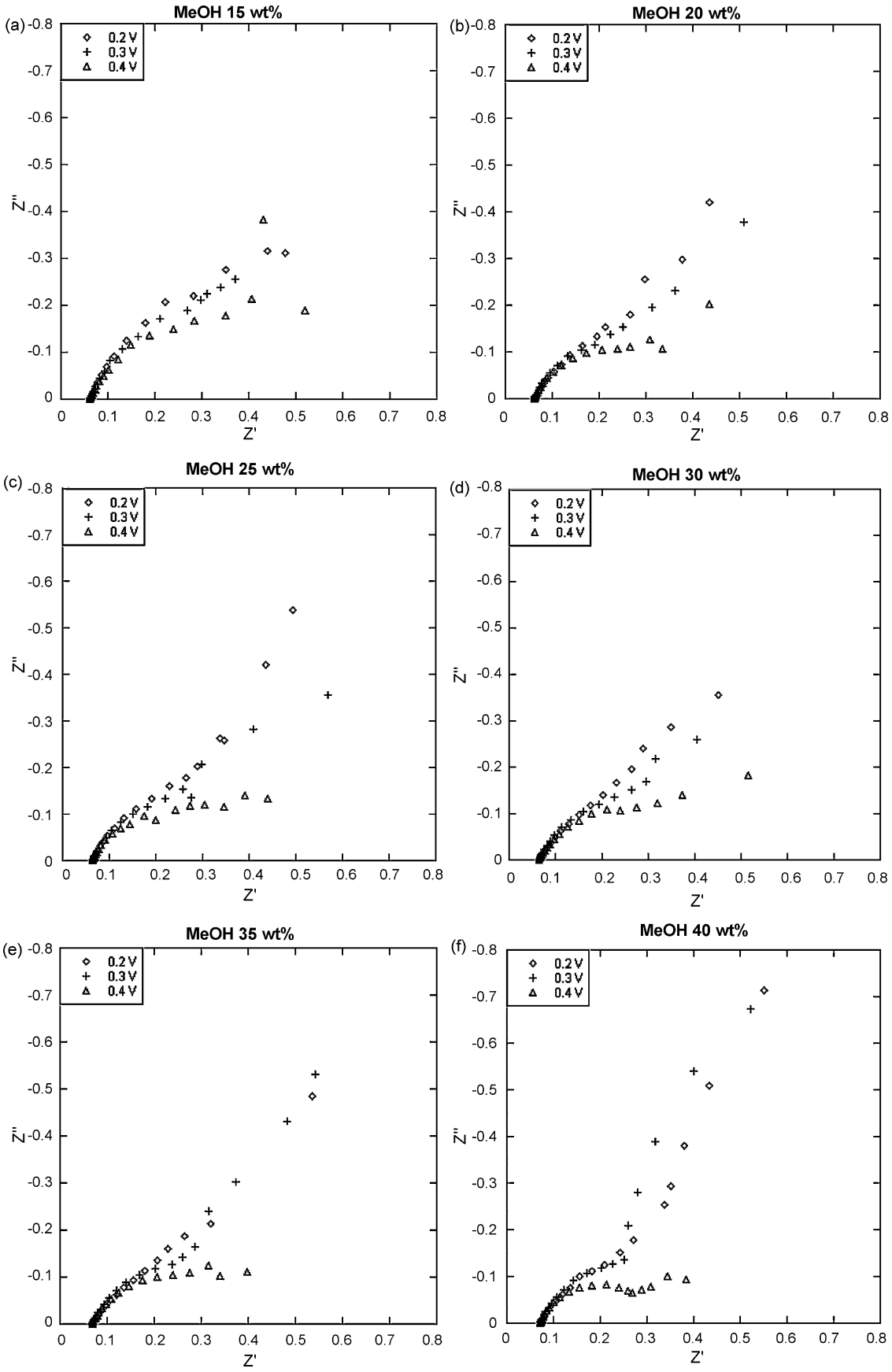

Fig. 11. Measurement of ac impedance from different applied voltage: (a) methanol 15 wt.% vapor; (b) methanol 20 wt.% vapor; (c) methanol 25 wt.% vapor; (d) methanol 30 wt.% vapor; (e) methanol 35 wt.% vapor; (f) methanol 40 wt.% vapor.

included the activation losses of the anode, it can be negligible due to very low losses, as seen in Table 1. In contrast with the behavior of methanol concentration, water concentration strongly affects anode overpotential. Since water is needed to oxidize methanol, the lack of water is seen to slow down the methanol oxidation [7].

3.3. Cathode activation loss

The cathode activation losses strongly depend on the methanol crossover and air-convection in the experiments. The cathode activation loss is not clear due to air-breathing in low concentration as it fluctuates (Fig. 10). In particular, the high methanol concentration of the anode significantly increases crossover rate to the cathode. The methanol crossover equation is as follows:

$$N_m = \frac{\lambda_m^I}{F} - \varepsilon^{1.5} D_m \frac{dc_m}{dz} \quad (5)$$

where C_m is the methanol concentration in the membrane. N is the methanol flux in the membrane. The D_m is diffusion coefficient of methanol [25]. The electro-osmotic drag coefficient (λ_m) of methanol is defined as the number of methanol molecules dragged by each proton membrane (CH_3OH/H^+), and is given by

$$\lambda_m = X|_{z=0}\lambda_w \quad (6)$$

where λ_w is the electro-osmotic drag coefficient for the water. X is the mole fraction in the membrane. The crossover rate is proportional to the concentration gradient between the anode and cathode. The cathodic methanol is oxidized to CO_2 and water.

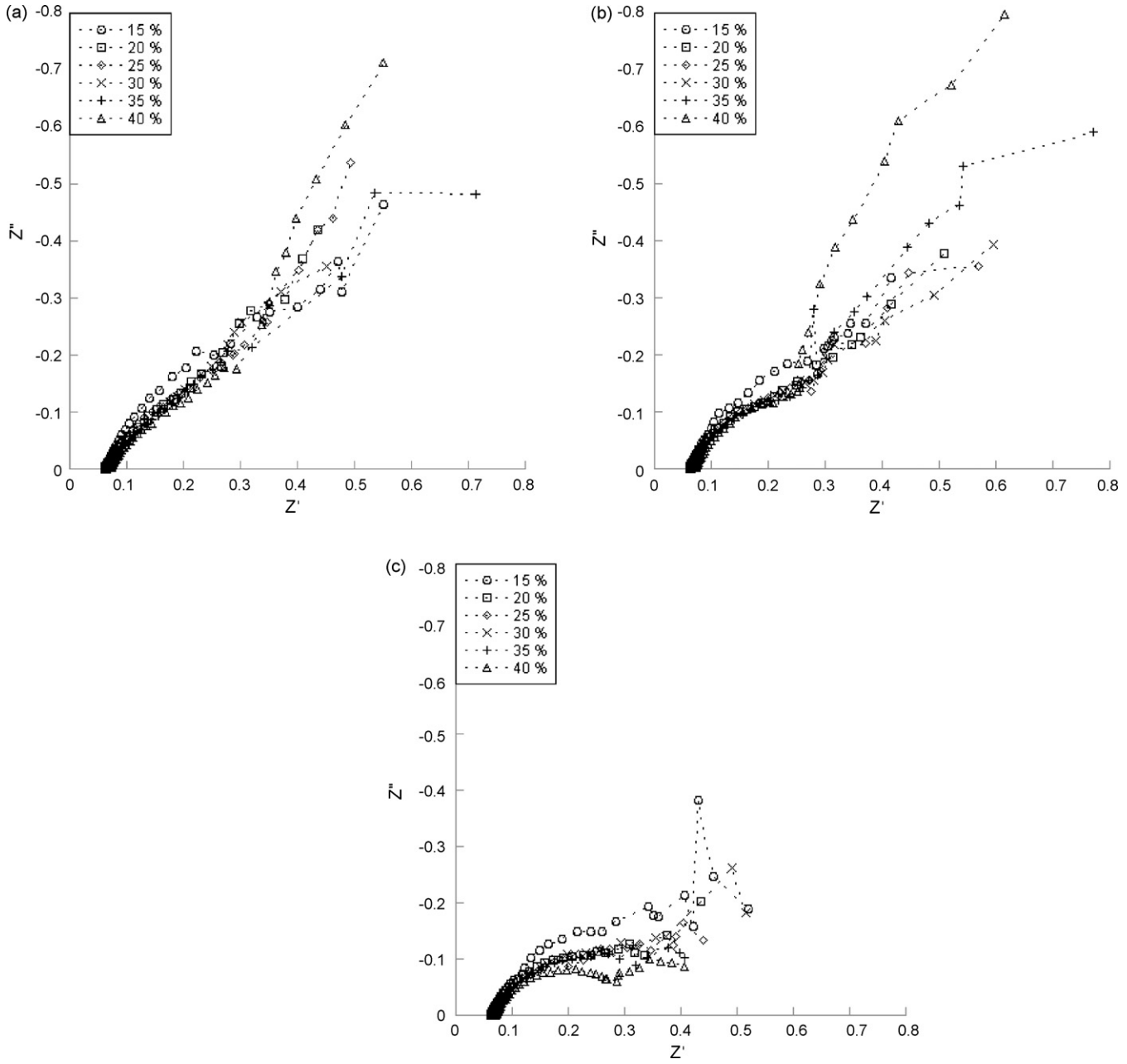

Fig. 12. Measurement of ac impedance from different methanol concentration: (a) 0.2 V; (b) 0.3 V; (c) 0.4 V. To obtain these curves, the graphs of Fig. 11(a)–(f) have been rearranged in terms of applied voltage.

Thus, the high methanol crossover generates water flooding, and affects the ionomer conductivity caused by back diffusion of the generated water at the cathode. The generated water obstructs the access of oxygen to the cathode catalyst layer. It directly affects the high activation losses at the cathode. Thus, high methanol concentration leads to high activation losses at the cathode. Within the whole current range, the activation losses for 40 wt.% is the highest; in 8 mol, the voltage loss of the anode is 0.15 V at 0.09 A, but the voltage loss of the cathode is 0.2 V at same current. Over 40 wt.%, the voltage loss of the cathode is found to be dominant.

3.4. Impedance analysis

At high frequency, according to the methanol concentration and the applied voltage, Table 1 shows the IR loss. IR loss increased with the rise of methanol concentration. Because of room temperature experiments, the temperature of the cathode is almost stable (42–45 °C). Interestingly, the water content of the fuel gas is directly proportional to the IR losses. Therefore, with increasing water content in low methanol concentrations that is a decline in the IR loss. Although back diffusion of water affects the ionomer conductivity under a high crossover rate, the generated water did not exert any influence on the membrane resistance. The gas diffusion layer of the cathode does not maintain the generated water. This phenomenon can be attributed to two factors. One is the high opening ratio (90%) that leads to rapid evaporation of the generated water due to the high fuel crossover rates. Also, in the operating temperature, the used hydrophobic gas diffusion layer does not function as water reservoir for back-diffusion which relies strongly on the GDL temperature at the cathode [26].

As stated in setup and measurement, we employed high amplitude (100 mV) for measuring impedance spectra in the high current region. Basically, as seen from the polarization curves and the overpotential of anode and cathode from Figs. 8–10, the polarization response of the fuel is quite linear at the measurement points of impedance spectra. Therefore, we believe that usage of such high amplitude for impendence spectra can at least provide useful trend of impedance change even though not accurate. The Warburg effect dominates in the high current region, as shown in Figs 11 and 12Figs. 11(a)-(f) and 12(a). In particular, the Warburg of high methanol concentration is dominant as shown in Fig. 11(e) and (f). This reveals that water generation of the cathode hinders the kinetics in the high current region. Consequently, the Faradaic impedance of the cathode increases due to flooding of the cathode. Secondly, the methanol crossover severely deteriorates the flooding at the cathode. This phenomenon can be seen clearly in high methanol concentration. Although the anode requires a high concentration in Fig. 11(e/0.4 V) and (f/0.4 V), the crossover increases at the cathode as seen in Fig. 11(e/0.2 V), 11(f/0.2 V) and 12(a). In these conditions, the mass transport effect is dominant. On the contrary behavior of PEM fuel cells, the Faradaic impedance is increased regardless of the methanol concentration with the rise of current [27]. Figs. 11(f) and 12(c) reveal that the Faradaic impedance of 40 wt.% is low. Because of low current region, the anode activation loss is also low, and the generated water of the cathode does not affect the kinetics. However, the activation losses at 15 wt.% is high within the whole current density.

4. Conclusion

The experimental concepts identified the optimal operational conditions of vapor-fed DMFCs, and the subsequent analysis by measuring the characteristic behavior that was obtained through impedance analysis. The IV polarization curves confirm the optimal concentration (25–30 wt.%) for vapor-fed and air-breathing DMFCs. The peak power was 14 mW cm^2. At the same time, we measured activation losses of the anode and cathode. The anode catalyst layer becomes more efficient when supplied with a high methanol concentration. The anode activation loss is high in low methanol concentration, but the cathode activation loss is high in high methanol concentration. In EIS measurements, high methanol concentrations are more susceptible to crossover at the cathode. According to the Faradaic loops, the methanol crossover deteriorates water-flooding at the cathode. Thus, the water-flooding hinders the transport of air (oxygen) to the cathode catalyst layer. Consequently, the activation loss of the cathode increases due to the high methanol concentrations. The water contents of the fuel gas directly affect the IR losses which are found to increase. IR loss increases under low methanol concentrations.

Acknowledgements

This work was sponsored by Samsung Advanced Institute of Technology, SNU-IAMD and Brain Korea 21 program.

References

[1] C.-C. Yang, S.-J. Chiu, C.-T. Lin, J. Power Sources 177 (2008) 40–49.
[2] J.-Y. Park, J.-H. Lee, J. Lee, S. Han, I. Song, J. Power Sources 179 (2008) 1–8.
[3] Y.H. Pan, J. Power Sources 161 (2006) 282–289.
[4] V. Baglio, A. Stassi, F.V. Matera, A. Di Blasi, V. Antonucci, A.S. Arico, J. Power Sources 180 (2008) 797–802.
[5] Y.H. Chan, T.S. Zhao, R. Chen, C. Xu, J. Power Sources 178 (2008) 118–124.
[6] M.A. Abdelkareem, N. Morohashi, N. Nakagawa, J. Power Sources 172 (2007) 659–665.
[7] S. Eccarius, B.L. Garcia, C. Hebling, J.W. Weidner, J. Power Sources 179 (2008) 723–733.
[8] H.-T. Kim, T.V. Reschentenko, H.-J. Kweon, J. Electrochem. Soc. 154 (2007) B1034–B1340.
[9] J. Nordlund, G. Lindergh, J. Electrochem. Soc. 149 (2002) A1107–A1113.
[10] S. Reichman, T. Duvdevani, A. Aharon, M. Philosoph, D. Golodnitsky, E. Peled, J. Power Sources 153 (2006) 228–233.
[11] B.K. Kyo, B. Bae, M.A. Scibioh, J. Lee, H.Y. Ha, J. Power Sources 142 (2005) 50–55.
[12] S.B. Adler, B.T. Henderson, M.A. Wilson, D.M. Taylor, R.E. Richards, Solid State Ionics 134 (2000) 35–42.
[13] G. Li, P.G. Pickup, Electrochim. Acta 49 (2004) 4119–4126.
[14] A. Küver, I. Vogel, W. Vielstich, J. Power Sources 52 (1994) 77–80.
[15] H.K. Kim, J. Power Sources 162 (2006) 1232–1235.
[16] W. Lee, H. Kim, T.K. Kim, H. Chang, J. Membr. Sci. 292 (2007) 29–34.
[17] J.H. Yang, Y.C. Bae, J. Electrochem. Soc. 155 (2008) B194–B199.
[18] S. Eccarius, T. Manurung, C. Ziegler, J. Electrochem. Soc. 154 (2007) B852–B864.
[19] W. He, T. Van Nguyen, J. Electrochem. Soc. 153 (D149) (2006) A185–A195.
[20] B. Bae, B.K. Kho, T.H. Lim, I.H. Oh, S.A. Hong, H.Y. Ha, J. Power Sources 158 (2006) 1256–1261.
[21] J. Liu, G. Sun, F. Zhao, G. Wang, G. Zhao, L. Chen, B. Yi, Q. Xin, J. Power Sources 133 (2004) 175–180.
[22] Z. Qi, A. Kaufman, J. Power Sources 110 (2002) 177–185.
[23] R. Jiang, D. Chu, J. Electrochem. Soc. 151 (2004) A69–A76.
[24] R. O'Hayre, S.W. Cha, W. Collela, F.B. Prinz, Fuel Cell Fundamentals, Wiley, 2005.
[25] J. Ge, H. Liu, J. Power Sources 163 (2007) 907–915.
[26] C. Xu, T.S. Zhao, J. Power Sources 168 (2007) 143–153.
[27] S.W. Cha, R. O'hayre, Y.I. Park, F.B. Prinz, J. Power Sources 161 (2006) 138–142.